JOURNAL OF THERMOPHYSICS AND HEAT TRANSFER
Vol. 9, No. 3, July–September 1995

Prediction of Vibrational Relaxation in Hypersonic Expanding Flows Part 2: Results

Stephen M. Ruffin*
Georgia Institute of Technology, Atlanta, Georgia 30332-0150

This article examines the range of applicability and performance of the Landau–Teller vibrational relaxation model and a simplified anharmonic model in expanding flows. The simplified relaxation model allows both non-Boltzmann population distributions and includes anharmonic transition rates and energy transfer. A coupled set of vibrational transition rate equations and quasi-one-dimensional fluid dynamic equations is solved. The calculations are compared with experimental results obtained in nozzles. The predictions of the detailed master equation solver are in excellent agreement with experimental results. Although the simplified anharmonic model requires significantly less computational time than the master equation solver, it gives good agreement with the detailed solver and with experimental test results.

Nomenclature

E_v = energy in level v per molecule, erg
$(e_{\text{vib}})_m$ = vibrational energy of species m per unit mass (relative to ground state), erg/g
N = number density of gas mixture, cm^{-3}
p = static pressure, dyne/cm^2
T = translational temperature, K
T_{vib} = vibrational temperature based on energy in vibrational mode, K
T_{vib_v} = vibrational temperature based on population at levels v and $v + 1$, K
u = streamwise flow velocity, cm/s
v = vibrational quantum level
x = streamwise spatial coordinate, cm
η_s = mole fraction of species s
τ = vibrational relaxation time, s
ϕ = local acceleration factor, $\dot{e}_{\text{vib}}/e_{\text{vib}}^{\text{LT}}$
$\bar{\phi}$ = constant overall acceleration factor

Subscripts
E = thermal equilibrium condition
LT = Landau–Teller model
m = diatomic chemical species m
s = chemical species s
t = stagnation condition
v = vibrational quantum level v

Superscripts
LT = Landau–Teller model
VT = vibration-translation collisions
VV = vibration-vibration exchange collisions

Introduction

IN Part 1 of this study,[1] the inability of the Landau–Teller relaxation model to accurately predict some details of the vibrational relaxation process in expanding flows was discussed. A simplified relaxation model was proposed to give more accurate predictions in expansions. The simplified model developed in Part 1 is designed to be much more computationally efficient than a detailed master equation solver, while maintaining reasonable accuracy over a wide range of conditions. In the present study calculations are performed with the simplified anharmonic model and with the Landau-Teller model. These results are compared with experimental data and with results obtained by solving the vibrational master equation.

The vibrational relaxation processes of N_2 and CO in cooling flows are studied. For the detailed calculations, a coupled set of vibrational master equations and quasi-one-dimensional fluid dynamic equations is solved. Vibration-translation (V-T) transition rates are computed from a modified version of the Schwartz, Slawsky, and Herzfeld[2] (SSH) theory, and vibration-vibration (V-V) exchange rates are computed by considering both long-range and short-range intermolecular forces. The transition rates are validated with available experimental data and other theoretical models. The reader is referred to a prior study by Ruffin[3] for a detailed description of the quasi-one-dimensional solver and the transition rates. The quasi-one-dimensional solver is used to predict the steady-state flow in nozzles and to conduct idealized studies of vibrational relaxation under isothermal conditions.

The present computational schemes are compared with experimental data obtained in expanding nozzles. Relaxation predictions are compared with the most reliable experimental results, which use direct measurement techniques for population distributions and have very low levels of impurities in the test gas. Anharmonic and harmonic oscillator predictions are also compared in external flows around a blunt re-entry vehicle.

The present study also seeks to address three questions related to the simplified anharmonic model:

1) How accurate is the model compared to master equation solutions and experimental data?

2) What is its range of applicability?

3) Is the computational requirement prohibitive for use in multidimensional flow codes? The accuracy of the model for a wide range of conditions in isothermal relaxations is studied in the next section. The range of applicability is also discussed later in that section. In the subsequent section the model is compared to experimental data and master equation solutions in nonisothermal gasdynamic flows. Both of the next two sections include assessments of the model's computational requirements.

Isothermal Relaxation Results

Many of the important features of detailed vibrational relaxation can be investigated through isothermal, constant vol-

Presented as Paper 94-0456 at the AIAA 32nd Aerospace Sciences Meeting, Reno, NV, Jan. 10–13, 1994; received April 1, 1994; revision received Sept. 30, 1994; accepted for publication Nov. 4, 1994.

*Assistant Professor, School of Aerospace Engineering. Member AIAA.

ume simulations. In isothermal simulations we consider a slug of gas in a constant volume "box" that initially has an equilibrium Boltzmann population distribution. At time $t = 0$, the translational temperature of the gas is set to and fixed at some different temperature T. Vibrational transitions are allowed to proceed so that the gas relaxes to an equilibrium Boltzmann distribution at T. In this section the predictions of the simplified anharmonic relaxation model in isothermal relaxations are compared to results obtained by solving the vibrational master equations.

Cooling simulations involve relaxation of the test gas from a high vibrational temperature to equilibrium at a lower T. The relaxation process is similar to that which occurs in expanding flows in that the vibrational temperature is higher than the translational temperature, i.e., $T_{vib}/T \geq 1$. In the first case studied, N_2 at $p = 1$ atm is relaxed from an initial Boltzmann distribution at 6000 K to equilibrium at $T = 1000$ K. The vibrational temperature predictions are given in Fig. 1. The anharmonic relaxation model provides excellent agreement in vibrational temperature with the master equation solution. The evolution of the population distributions at various times in the relaxation is shown on Fig. 2. The present simplified model also agrees with the predicted distribution from the master equation solver.

In addition to the previous case, a number of other solutions were generated for several translational temperatures and initial vibrational temperatures. One way to quantify the acceleration of vibrational relaxation relative to the Landau–Teller model is to compute a local acceleration factor ϕ, which is defined as

$$\phi = \dot{e}_{vib}/\dot{e}^{LT}_{vib} \tag{1}$$

where $\dot{e}_{vib} = d(e_{vib})_m/dt$ is the local rate of vibrational energy transfer predicted by either the master equation solver or the anharmonic model, and $\dot{e}^{LT}_{vib}$ is the local energy transfer rate that would have been predicted by the Landau–Teller model. ϕ is a *local* acceleration factor because it is computed at every step in the relaxation. Therefore, ϕ is the ratio of the anharmonic oscillator energy transfer rate to the rate that would have been predicted by the Landau–Teller model at the same conditions. In this way it differs from the *global* $\bar{\phi}$ referred to in many previous experiments, which attempted to determine one constant acceleration factor for the entire relaxation process.

The local acceleration factor for N_2 is shown as a function of T_{vib}/T for several translational temperatures in Fig. 3. The results are appropriate for a wide variety of flow conditions, but do not apply in the short time period before V-V exchange quasiequilibrium has been established. The energy transfer during that short time period is a function of the initial distribution of the relaxation. The results shown in Fig. 3 are appropriate for the remaining part of the relaxation process, regardless of the initial condition. The results shown in Fig. 3 are quite general because for a given collision pair the value of ϕ is only a function of T and T_{vib}/T and not a function of the initial condition (except during the initial V-V exchange transient). The local acceleration factor predicted by the detailed master equation solver and ϕ predicted by the anharmonic model developed in Part 1 of this study[1] are presented in Fig. 3.

We see that in heating environments, i.e., $T_{vib}/T < 1$, ϕ is not substantially different from unity. Note that $\phi = 1$ corresponds to a condition in which Landau–Teller is accurate. Thus, for temperatures in the range 1000 K $\leq T \leq$ 5000 K the Landau–Teller relaxation model is a reasonable approximation for relaxations in heating environments such as those in postshock flows. However, in cooling relaxations, i.e., $T_{vib}/T > 1$, vibrational relaxation can be significantly faster than Landau–Teller predicts, especially for $T_{vib}/T > 2.5$. The factor ϕ is 1–2 orders of magnitude greater than unity for some conditions. Clearly, the Landau–Teller model is inadequate for predicting the energy transfer rate in flows in which the vibrational temperature is much greater than the translational temperature.

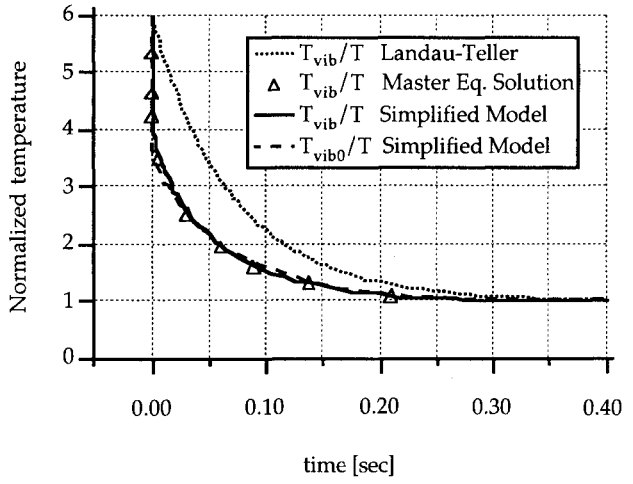

Fig. 1 Comparison of vibrational temperatures predicted by the simplified anharmonic relaxation model to master equation results for relaxation of N_2 at $p = 1$ atm from 6000 to 1000 K.

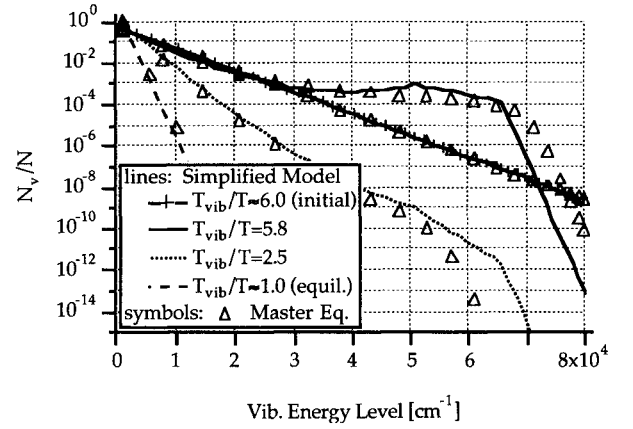

Fig. 2 Comparison of population distributions predicted by the simplified anharmonic relaxation model to master equation results for relaxation of N_2 at $p = 1$ atm from 6000 to 1000 K.

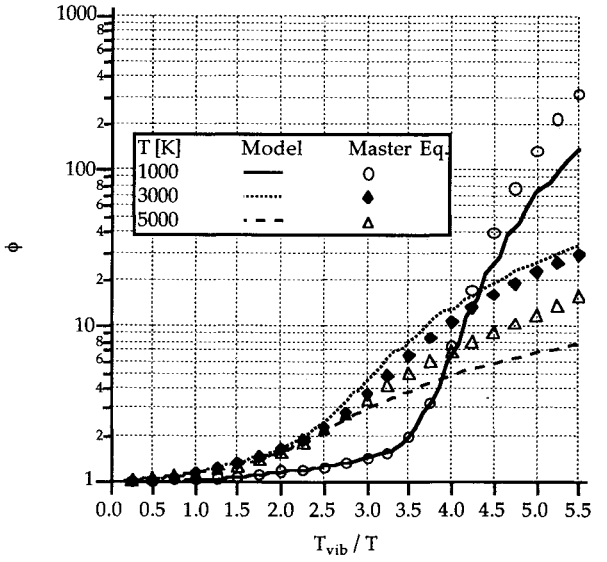

Fig. 3 Comparison of ϕ predicted by the simplified anharmonic relaxation model to master equation results for relaxation of N_2.

The values of ϕ predicted by the simplified relaxation model are compared to the master equation results in Fig. 3. The simplified model is found to give good agreement with the master equation results for all conditions in which the V-T rates dominate the energy transfer. The agreement is generally within 30% for $0 < T_{vib}/T \leq 4.5$. For more extreme cases of thermal nonequilibrium (i.e., $T_{vib}/T > 4.5$), the energy transferred directly by V-V collisions becomes significant. Consequently, the predicted energy transfer rate of the anharmonic relaxation model (which only considers V-T energy transfer), is too low. However, even for these extreme cases of thermal nonequilibrium, the relaxation rate predicted by the present model is much more accurate than the Landau–Teller rate (which corresponds to $\phi = 1$). The range of applicability of the present anharmonic model is much wider than that for the Landau–Teller model. The present model gives reasonable agreement with the master equation solution for relaxation of nitrogen with conditions generally in the range $0 < T_{vib}/T \leq 4.5$.

It should be noted that although the simplified anharmonic model gives good agreement with the master equation solver, it requires significantly less computational time to calculate. Each of the isothermal simulations with the master equation solver required approximately 1500 s on a Cray Y-MP computer, whereas the simplified model required only 4 s. Because the simplified model requires over two orders of magnitude less computational time to compute, it is much more practical for use in conventional time-marching, multidimensional flow solvers. The simplified model does, however, require more computational effort than the Landau–Teller formulation, which consumed approximately 1 s of computational time per isothermal simulation.

Nozzle Flow Results and Validation

Overview

Nozzle flow experiments have been conducted that attempt to quantify the faster vibrational relaxation rate in nozzles compared to postshock flows. Many of these experiments used methods that have substantial uncertainty and error of their vibrational temperature measurements.[3] The errors are due to impurities, indirect vibrational temperature measurement techniques, and effects of shock diaphragms. Many of the methods used to measure vibrational temperature are based on the assumption that the population distributions throughout the expansion are Boltzmann. However, we have seen that for conditions in which the vibrational temperature is much greater than the translational temperature, the distribution is far from Boltzmann. The assumption of a Boltzmann distribution in a nozzle has been shown to introduce a systematic error in the inferred vibrational temperatures.[4] The validation experiments chosen in this study make no a priori assumption of the population distribution, but instead measure the distribution of a number of vibrational quantum levels. The measurement of the population distribution allows direct comparison of the results to the present master equation solutions and to the simplified anharmonic relaxation model.

The calculations in this study were conducted with a quasi-one-dimensional solver and with a two-dimensional time-marching, real-gas code. The two-dimensional code solves the Navier–Stokes equations and is a modified version of a code developed by Palmer.[5] The modifications to the code are discussed by Sharma et al.[6] and Ruffin.[3] The effects of the boundary-layer growth on the inviscid core were included in the present calculations of each of the nozzle flow cases.

Bender Nozzle Experiment

The first set of tests examines vibrational relaxation of mixtures of carbon monoxide and argon in a supersonic expansion. This experiment was conducted in an arcjet wind tunnel and is described completely by Bender.[7] The test gas is a mixture of argon with 5–20% of CO and the nozzle is composed of aluminum. Vibrational population distributions are determined from measurements of the first overtone vibration-rotation radiative emissions.

The stagnation conditions and CO mole fractions for the five test cases are shown in Table 1. Because the maximum temperature is 3000 K, the CO does not dissociate for any of the cases and the chemical composition is frozen.

Computed values of T_{vib} and T are shown in Fig. 4 for case B. The translational temperature decreases throughout the nozzle while the temperature based on energy in vibration T_{vib} "freezes" soon after the throat. The decreasing translational temperature is driven primarily by fluid dynamic effects caused by the increasing area ratio of the nozzle. Because the translational temperature decreases so rapidly, the vibrational transition rates also decrease quickly. The vibrational relaxation appears to be frozen because it is occurring so slowly and because it does not make progress toward thermal equilibrium. Park[8] shows that vibrational freezing occurs approximately where

$$\frac{1}{e_{vib_E}} \frac{de_{vib_E}}{dx} \geq \frac{1}{u\tau_{LT}} \tag{2}$$

This is a form of Bray's sudden freezing criterion.[9] The translational temperature at the nozzle exit is approximately 380 K, and so the degree of thermal nonequilibrium is large with $T_{vib}/T \approx 6$ for this case. The value of T_{vib} predicted by the master equation is virtually the same as that predicted by the Landau–Teller model. For this extreme case of thermal nonequilibrium the rate of energy transfer for the anharmonic master equation is much faster than that for the Landau–Teller model at the exit. However, this anharmonic acceleration happens after vibrational freezing occurs. The sudden freezing criterion is satisfied at $x = -0.33$ cm, while the nozzle throat is at $x = 0.0$ cm. Thus, for this case, the rapid flow acceleration that begins ahead of the throat induces very early vibrational freezing.

The computed vibrational temperatures for case B are compared with the experimental measurement in Fig. 5. Although

Table 1 Test conditions for Bender nozzle experiments

Case	T_r, K	p_r, dyne/cm^2	η_{CO}
A	2000	6.75838×10^6	0.101
B	2400	7.13328×10^6	0.093
C	2350	6.96103×10^6	0.170
D	2300	7.10288×10^6	0.199
E	3000	6.99143×10^6	0.056

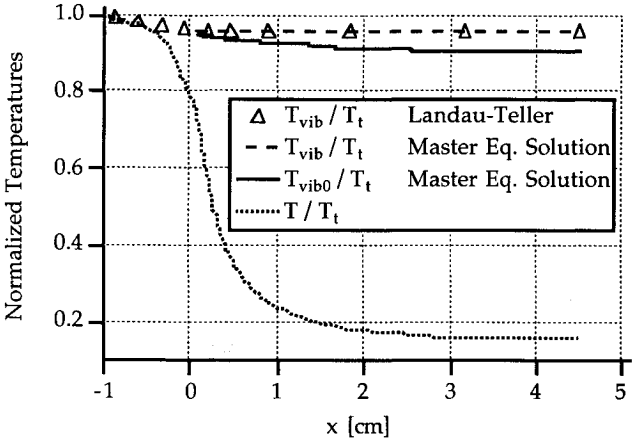

Fig. 4 Comparison of computed temperatures for the Landau–Teller model and master equation solution for case B of the Bender experiment.

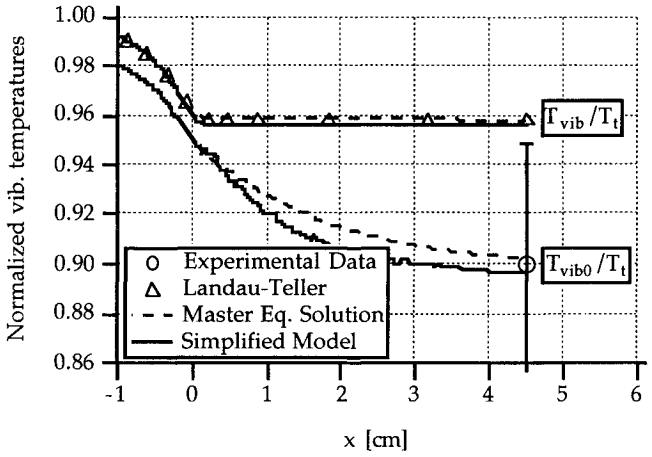

Fig. 5 Comparison of experimental and computational vibrational temperatures for case B of the Bender experiment.

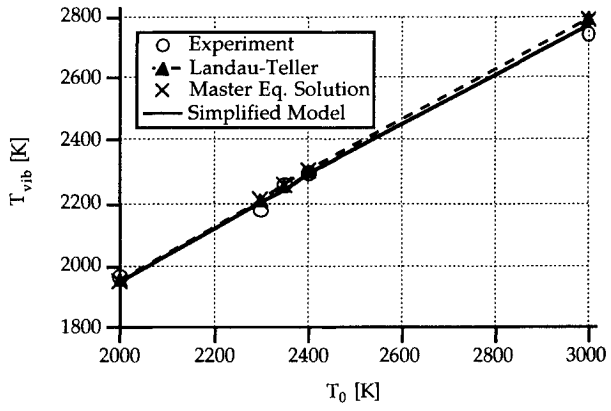

Fig. 6 Comparisons of experimental and computational vibrational temperatures at the nozzle exit for all cases of the Bender experiment.

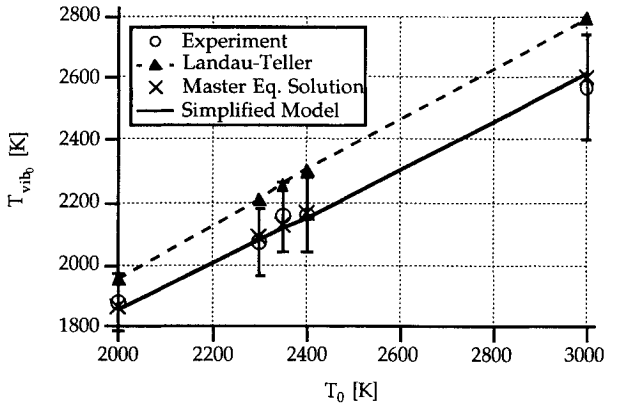

Fig. 7 Comparisons of experimental and computational ground state vibrational temperatures at the nozzle exit for all cases of the Bender experiment.

the three computational schemes give virtually the same T_{vib}, only the master equation and the simplified anharmonic relaxation models give good agreement with the experimental result for the ground state vibrational temperature. T_{vib_0} is significantly lower than T_{vib} because of the non-Boltzmann distribution that exists at the nozzle exit.

The vibrational temperature results found in case B are typical of those for all five of the test conditions. Figures 6 and 7 show T_{vib} and T_{vib_0}, respectively, at the nozzle exit as a function of stagnation temperature for the test conditions shown in Table 1. From Fig. 6 we see that both the harmonic oscillator and anharmonic oscillator methods give excellent agreement with the experimental results for the energy in vibration at the nozzle exit. However, Fig. 7 demonstrates

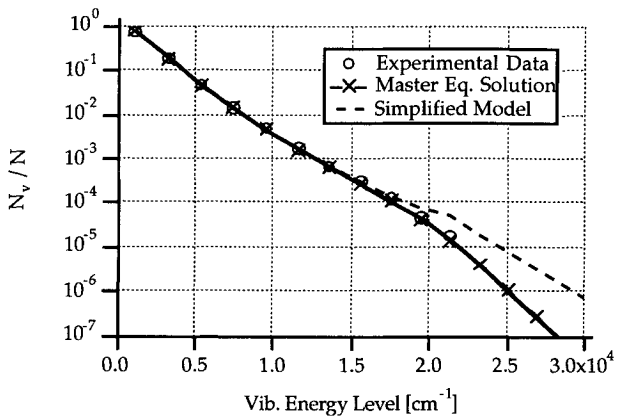

Fig. 8 Comparison of experimental and computational population distribution at the nozzle exit for case B of the Bender experiment.

that the Landau–Teller model gives poor agreement with the value of the ground state vibrational temperature. The master equation solver and the simplified anharmonic relaxation model both give excellent agreement with the experimental results throughout the temperature range. The excellent agreement of the simplified model is especially encouraging, because it requires little more computational time to compute than the Landau–Teller model, and almost two orders of magnitude less time than the master equation solution.

Figure 8 shows experimental and computational results for the normalized population distributions at the nozzle exit for case B. In this figure we observe a subtle upward curvature of the distributions, which indicates overpopulation of the midquantum levels. This overpopulation is due to rapid V-V exchange transitions. The upward curvature is slight because the test gases used are diluted CO-Ar mixtures rather than pure CO. The CO-Ar V-T transitions diminish the effects of the CO V-V exchanges by tending to cause more rapid de-excitations of the mid and upper quantum levels. The master equation solution is found to give excellent agreement with the experimental results for all quantum levels and all test conditions. This excellent agreement allows confidence in the V-T and V-V transition rates used. The simplified anharmonic relaxation model gives excellent agreement with the experimental results for the first eight quantum levels for the test conditions. The agreement begins to diminish for higher quantum levels, but the population in these levels decreases rapidly. The overall agreement of the simplified model with the experimental results is good and the discrepancies observed are probably due to the approximation used to determine the appropriate values of $\bar{v}_1^*$ and $\bar{v}_2^*$ to use in gas mixtures. The expressions used to determine $\bar{v}_1^*$ and $\bar{v}_2^*$ are given in Refs. 1 and 3.

EAST Facility Nozzle Experiment

In this second experiment, vibrational relaxation of nitrogen is studied in a converging–diverging nozzle. This test was conducted in the NASA Ames Research Center Electric Arc-Driven Shock Tube (EAST) Facility. The basic capabilities of this facility are described by Sharma et al.,[10] and the configuration for the present studies is given by Sharma et al.[11] and Gillespie et al.[12] The test gas is prepurified N_2 with a total estimated impurity level of <10 ppm, and the nozzle and diaphragm are made of aluminum. The nominal conditions in the reservoir upstream of the nozzle are shown in Table 2 for the cases tested.

Vibrational population distributions of the lower levels are measured experimentally using Raman scattering spectroscopy. This technique is described by Sharma et al.[16] and Gillespie et al.[20]

In Fig. 9 experimental and computational ground state vibrational temperatures are compared for case A. For case A

Table 2 Test conditions for EAST Facility nozzle experiments

Case	T_t, K	p_t, dyne/cm^2	η_{N_2} in reservoir
A	2800	1.03352×10^8	1.0
B	5600	1.03352×10^8	0.987

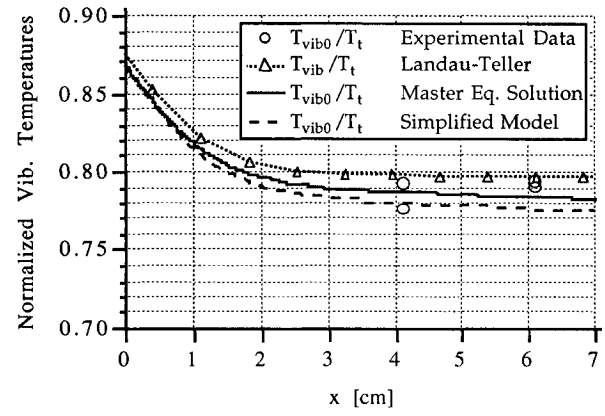

Fig. 9 Comparison of experimental and computational vibrational temperatures for case A of the EAST experiment.

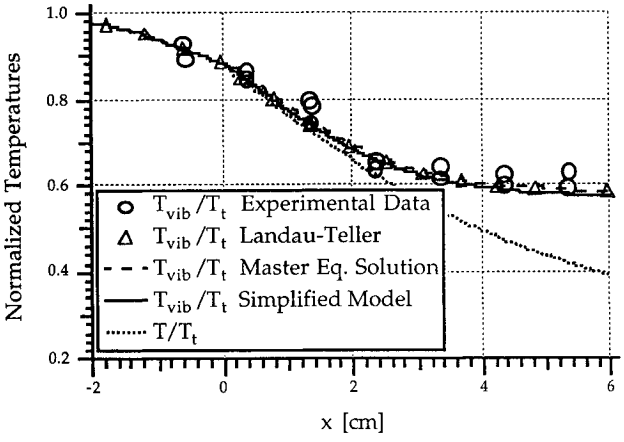

Fig. 10 Comparison of experimental and computational temperatures for case B of the EAST experiment.

the experimental vibrational temperatures are deduced from the integrated intensities of the $v = 0$ and $v = 1$. Thus, the measured vibrational temperature corresponds to T_{vib_0}. Both the harmonic oscillator and anharmonic schemes give good agreement with experimental data. For these conditions the population distribution is only slightly non-Boltzmann. The overall degree of thermal nonequilibrium is less extreme than in the Bender experiment. The difference among the three computational schemes and the experimental data is well within the uncertainty (50%) of the Millikan and White relaxation time correlation and the experimental uncertainty. The overall relaxation time for this expanding flow with a relatively mild degree of thermal nonequilibrium is not significantly different from that in a compressing flow at the same temperature.

For case B the vibrational temperatures are determined by applying a band-shape fitting technique to the Raman spectra for the first nine vibrational levels. In Fig. 10 these experimental and computed vibrational temperatures are compared as a function of streamwise distance. The Landau–Teller model, master equation solver, and the simplified anharmonic relaxation model all give good agreement with the experimental data. The anharmonic schemes predict only slightly faster relaxation than the Landau–Teller model for this case.

Re-Entry Flow

The previous two sections presented results along the centerline of nozzles. The quasi-one-dimensional calculations essentially followed one streamline of each of the flowfields. A multidimensional external flow around a realistic vehicle consists of many different streamlines, with each experiencing a different degree of thermochemical nonequilibrium. By computing such a multidimensional flow we can investigate vibrational relaxation under a wide variety of local conditions. In this section we investigate the flow around an axisymmetric vehicle at conditions typical of those experienced during Earth re-entry.

A schematic diagram of the flow structure often observed around a blunt re-entry vehicle was presented by Strawa et al.[13] and is also shown in Fig. 11. The shear layer divides the primary expansion region of the inviscid flow from the recirculating region behind the base of the vehicle. The recirculating region is difficult to numerically predict because the flow in this area is not necessarily steady and because the exact angle of the shear layer departure from the shoulder is sensitive to accuracy of boundary-layer predictions. Shadowgraph photographs obtained in ballistic range test facilities allow study of the shear layer and wake regions. These experiments indicate that the angle between the shear layer and the freestream direction is roughly 14 deg for blunt bodies at zero angle of attack.[13,14] In this article, vibrational relaxation is investigated by computing the inviscid flow around a generic vehicle with a blunt forebody and with the shear layer modeled by a wall that makes an angle of 14 deg with the freestream. The recirculating region is not computed because it normally has only a mild degree of thermal nonequilibrium,[3] and because it is difficult to accurately compute due to the fluid dynamic issues previously discussed. The geometry of the forebody is chosen to match that of the proposed Mars environmental survey (MESUR) probe.[15] The axisymmetric forebody geometry is shown in Fig. 12 and has a spherical nose radius of 0.5 m, followed by a 70-deg conical section.

The flow conditions chosen correspond to a freestream velocity of 5 km/s and an altitude of 80 km. The freestream gas is 100% N_2, but is allowed to dissociate and recombine in the flowfield around the vehicle. The flow is computed with the

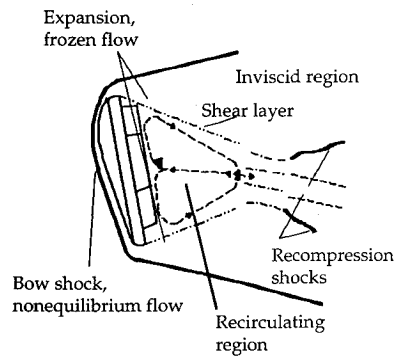

Fig. 11 Schematic of flow around a blunt re-entry vehicle.[13]

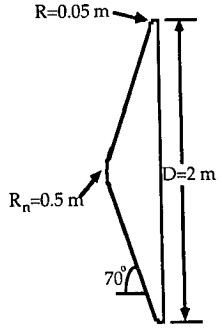

Fig. 12 Schematic diagram of axisymmetric, re-entry vehicle forebody.

two-dimensional real-gas, Navier–Stokes code described earlier. A body-fitted computational grid with 79 points in the streamwise direction and 41 points in the orthogonal direction is used. Both the Landau–Teller model and the simplified anharmonic relaxation model are utilized in the code. The full master equation formulation is too computationally intensive for this two-dimensional calculation. The two-dimensional code uses an explicit time-marching algorithm. It was found that when the simplified anharmonic model was employed, the value of ϕ varied quite slowly with the time coordinate. Thus, computational time was saved by computing ϕ every 10 time steps instead of every step. Also, ϕ was updated every 10 time steps by using the anharmonic model and the value of ϕ was held fixed between these intervals. This procedure was not found to increase the number of time steps required for convergence to a steady-state solution. Using this procedure, a converged solution with the anharmonic model required approximately 20% more computational time than with the Landau–Teller model.

In Fig. 13 results using the simplified anharmonic relaxation model are presented. On the bottom half of the figure T_{vib}/T is shown, and on the top half the local acceleration factor for N_2-N_2 collisions is presented. As expected, the most extreme thermal nonequilibrium occurs in the expansion region after the shoulder. We see that the anharmonic model predicts that $\phi_{N_2-N_2}$ is unity in the freestream and in the vibrational excitation region behind the bow shock. In the expansion region, $\phi_{N_2-N_2}$ is as high as 3.3.

The vibrational temperature based on energy in vibration T_{vib} was also compared for the Landau–Teller and anharmonic models. It was found that although $\phi_{N_2-N_2}$ is >1 in the expansion region, both the harmonic oscillator and anharmonic formulations gave essentially the same value of T_{vib} throughout the flowfield. As we observed in the previous nozzle cases, vibrational freezing occurs in the expansion before the faster anharmonic relaxation rate can significantly affect the energy in the vibrational mode. However, if we compare the anharmonic ground state vibrational temperature to that predicted by the Landau–Teller model, we see that the Landau–Teller model is in significant error in the expansion region. Figure 14 shows T_{vib_0} and T_{vib}, and in the expansion the Landau–Teller vibrational temperature is as much as 1200 K higher than that predicted by the anharmonic model. Electronic excitation and radiative emissions are strongly dependent on the vibrational population distribution,[16] which will be non-Boltzmann in the wake of re-entry vehicles. If we were to base radiative heating predictions on a Boltzmann distribution at T_{vib}, as predicted by the Landau–Teller model, then the predictions would be in substantial error.

We now compare Landau–Teller and anharmonic model results along one streamline of the flow. The streamline chosen is shown in Fig. 15. This line is the path that a particle just off the stagnation streamline will follow. The results are shown in Figs. 16–18. Several other cases were also computed, and for all flow conditions it was found that the an-

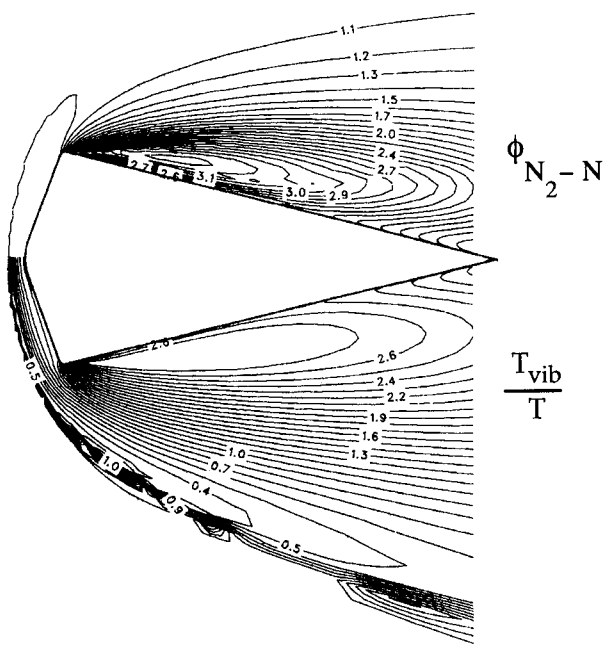

Fig. 13 Local acceleration factor for N_2-N_2 collisions (top) and T_{vib}/T (bottom) predicted by the anharmonic model for re-entry flow.

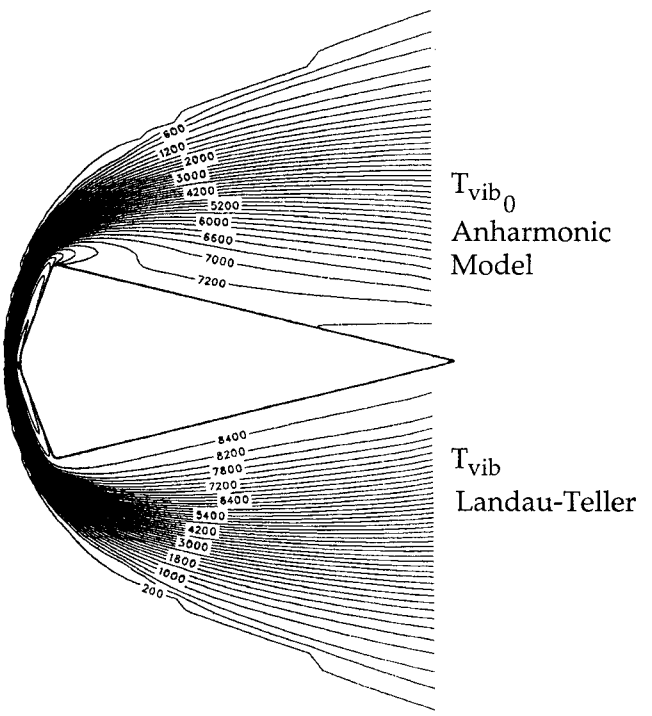

Fig. 14 Comparison of T_{vib_0} predicted by the anharmonic model (top) and T_{vib} predicted by the Landau–Teller model (bottom) for re-entry flow.

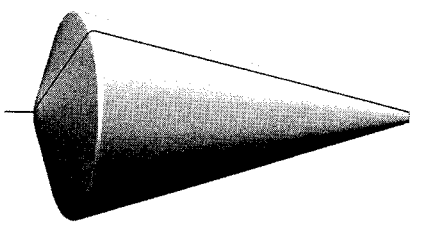

Fig. 15 Off-stagnation streamline (solid line) used for Figs. 16–18.

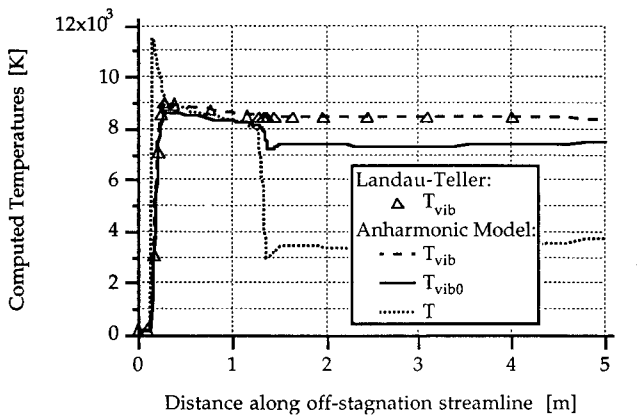

Fig. 16 Comparison of predicted temperatures along off-stagnation streamline for re-entry flow.

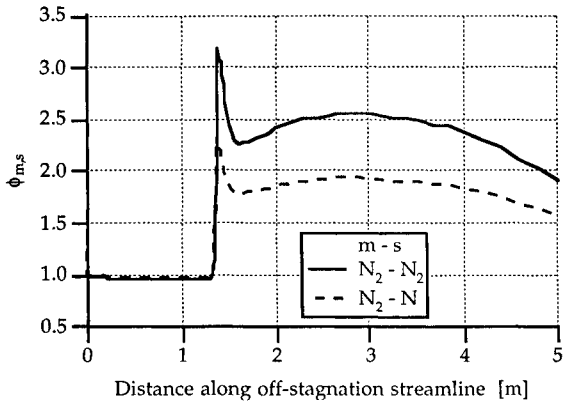

Fig. 17 Comparison of ϕ along off-stagnation streamline for re-entry flow.

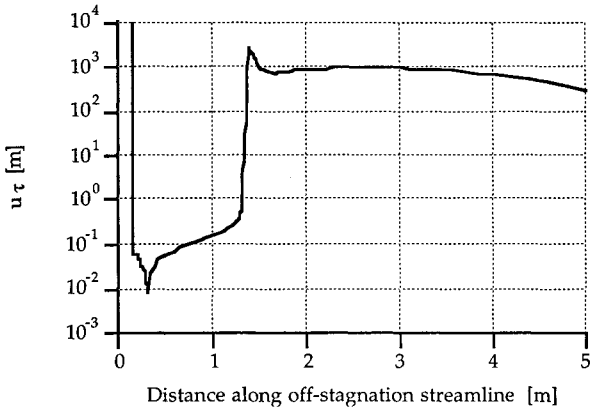

Fig. 18 Comparison of $u\tau$ along off-stagnation streamline for re-entry flow.

harmonic ground state vibrational temperature is significantly different from that predicted by the Landau–Teller model.[3] However, the vibrational temperature based on energy in vibration is virtually the same for the anharmonic and harmonic oscillator formulations.

We can further understand why T_{vib} is virtually the same for the two schemes by observing the local values of $u\tau$ shown in Fig. 18. The relaxation time is τ, and u is the convective speed, and so the distance required for the flow to achieve vibrational equilibrium is approximately $u\tau$. If we take a characteristic length of the flow to be the length of the geometry, i.e., $L \approx 5$ m, then just behind the bow shock $u\tau < L$. Because $u\tau < L$ in the postshock region, the rate of vibrational energy transfer is significant. However, in the expansion the convective speed increases and the vibrational relaxation time also increases dramatically. $u\tau$ becomes much larger than the characteristic length scale L. Because the rate of vibrational energy transfer is so slow, virtually no energy transfer occurs in the region of interest. Although the anharmonic energy transfer rate is over three times faster than the Landau–Teller rate (as shown in Fig. 17), the rate of vibrational energy transfer is so slow that the total energy in vibration is virtually unchanged within the length scale studied. For all of the reentry conditions studied, and all of the nozzle cases, it is found that vibrational freezing occurs before significant acceleration of the energy transfer rate occurs.

Conclusions

Quasi-one and two-dimensional viscous calculations have been performed to characterize vibrational relaxation in vibrationally cooling flows. The predictions of the detailed master equation solver are in excellent agreement with experimental results.

The degree of relaxation acceleration is found to be a function of both the translational temperature T and the ratio of vibrational-to-translational temperature T_{vib}/T. Non-Boltzmann population distributions are observed when $T_{vib}/T > 1$. Accurate predictions of radiative heating and vibration-dissociation coupling require knowledge of vibrational population distributions. In many cases the population distributions are far from Boltzmann, and if Landau–Teller results are used as a basis for radiative heating predictions, the results will be in substantial error. Anharmonic models, such as those developed herein, must be used for accurate modeling of these effects.

The local anharmonic energy transfer rate is shown to be an order of magnitude, or more, faster than the Landau–Teller model for extreme cases of thermal nonequilibrium. However, these large degrees of local acceleration are difficult to observe in gasdynamic flows because the vibrational energy becomes frozen in rapid expansions. The Landau–Teller model fails to predict non-Boltzmann population distributions for even moderate degrees of thermal nonequilibrium, but only fails to accurately predict the overall amount of energy in vibration for flows that both have high values of T_{vib}/T and for which $u\tau < L$. The flows of interest can only generate high values of T_{vib}/T through rapid expansions. However, such expansions also dramatically increase the value of $u\tau$, thereby causing vibrational freezing unless the characteristic length of interest is sufficiently large.

In summary, the Landau–Teller model gives fairly accurate predictions for the vibrational energy in most expansions, but fails to give accurate predictions of the distribution of vibrational energy. Anharmonic models are needed for accurate population distribution predictions and for the most accurate predictions of the energy transfer rate.

A simplified relaxation model is developed that allows both non-Boltzmann population distributions and includes anharmonic transition rates and energy transfer. Use of this model is demonstrated in internal nozzle flows and external flows around a re-entry vehicle. Although the model requires significantly less computational time than the master equation solver, it gives good agreement with the detailed solver and with experimental test results.

References

[1]Ruffin, S. M., "Prediction of Vibrational Relaxation in Hypersonic Expanding Flows Part 1: Model Development," *Journal of Thermophysics and Heat Transfer*, Vol. 9, No. 3, 1995, pp. 432–437.

[2]Schwartz, R. N., Slawsky, Z. I., and Herzfeld, K. F., "Calculation of Vibrational Relaxation Times in Gases," *Journal of Chemical Physics*, Vol. 20, No. 10, 1952, pp. 1591–1599.

[3]Ruffin, S. M., *Vibrational Energy Transfer of Diatomic Gases in Hypersonic Expanding Flows*, Ph.D. Dissertation, SUDDAR 635, Stanford Univ., Stanford, CA, June 1993.

[4]Center, R. E., and Caledonia, G. E., "Anharmonic Effects on the Rate of Relaxation of Vibrational Energy in Rapidly Expanding Flows," *Journal of Chemical Physics*, Vol. 57, No. 9, 1972, pp. 3763–3770.

[5]Palmer, G., "Enhanced Thermochemical Nonequilibrium Computations of Flow Around the Aeroassist Flight Experiment Vehicle," AIAA Paper 90-1702, June 1990.

[6]Sharma, S. P., Ruffin, S. M., Gillespie, W. D., and Meyer, S. A., "Vibrational Relaxation Measurements in an Expanding Flow Using Spontaneous Raman Spectroscopy," *Journal of Thermophysics and Heat Transfer*, Vol. 7, No. 4, 1993, pp. 697–703.

[7]Bender, D. J., "Measurement of Vibrational Population Distributions in a Supersonic Expansion of Carbon Monoxide," Ph.D. Dissertation, Dept. of Mechanical Engineering, Stanford Univ., Stanford, CA, March 1975; also Bender, D. J., Mitchner, M., and Kruger, C. H., "Measurement of Vibrational Population Distributions in a Supersonic Expansion of Carbon Monoxide," *Physics of Fluids*, Vol. 21, No. 7, 1978, pp. 1073–1085.

[8]Park, C., *Non-Equilibrium Hypersonic Aerothermodynamics*, Wiley, New York, 1990, pp. 185, 186.

[9]Bray, K. N. C., "Atomic Recombination in a Hypersonic Wind-

Tunnel Nozzle," *Journal of Fluid Mechanics*, Vol. 6, Pt. 1, 1959, pp. 1–32.

[10]Sharma, S. P., Gillespie, W. D., and Meyer, S. A., "Shock Front Radiation Measurements in Air," AIAA Paper 91-0573, Jan. 1991.

[11]Sharma, S. P., Ruffin, S. M., Gillespie, W. D., and Meyer, S. A., "Vibrational Relaxation Measurements in an Expanding Flow Using Spontaneous Raman Spectroscopy," *Journal of Thermophysics and Heat Transfer*, Vol. 7, No. 4, 1993, pp. 697–703.

[12]Gillespie, W. D., Bershader, D., Sharma, S., and Ruffin, S. M., "Raman Scattering Measurements of Vibrational and Rotational Distributions in Expanding Nitrogen," AIAA Paper 93-0274, Jan. 1993; also Gillespie, W. D., "Raman Scattering Measurements of Vibrational Relaxation in Expanding Nitrogen," Ph.D. Dissertation, Dept. of Aeronautics and Astronautics, Stanford Univ., Stanford, CA, 1993.

[13]Strawa, A. W., Park, C., Davy, W. C., Babikian, D. S., Craig, R. A., and Venkatapathy, E., "Proposed Radiometric Measurement of the Wake of a Blunt Aerobrake," *Journal of Spacecraft and Rockets*, Vol. 29, No. 6, 1992, pp. 765–772.

[14]Park, C., and Davies, C. B., "Raked Circular-Cone Aerobraking Orbital Transfer Vehicle," Patent 4903918, U.S. Patent Office, Feb. 1990.

[15]Tauber, M., Henline, W., Chargin, M., Papadopoulos, P., Chen, Y., Yang, L., and Hamm, K., "MESUR Probe Aerobrake Preliminary Design Study," AIAA Paper 92-2952, July 1992.

[16]Nadler, I., and Rosenwaks, S., "Studies of Energy Transfer Processes in Triplet States of N_2. 1. Energy Pooling by Vibrationally Selected $N_2(A^3\Sigma_u^+, v)$ Molecules," *Journal of Chemical Physics*, Vol. 83, No. 8, 1985, pp. 3932–3940.